3D Exterior Soundfield Capture Using Pressure and Gradient Microphone Array on 2D Plane

Lachlan Birnie, Prasanga N. Samarasinghe, and Thushara D. Abhayapala
Research School of Engineering, College of Engineering and Computer Science
The Australia National University, Canberra, Australia

***Abstract*—Two-dimensional (2D) planar array of first order microphones have been utilised in spherical harmonic decomposition based interior soundfield analysis. This paper proposes an efficient method in designing two-dimensional planar arrays of first order microphones that are capable of completely capturing three-dimensional (3D) spatial exterior soundfields. First order microphones are utilised within the array for measurements of pressure gradients, allowing the microphone array to capture soundfield components that conventional planar omni-directional microphone arrays are unable to detect. While spherical microphone arrays are capable of detecting all soundfield components, they have drawbacks in feasibility due to their 3D geometric configuration. The proposed planar array of first-order microphone provides the same functionality as a large spherical array which needs to encompass all sound sources while having a scalable geometry that lies purely in a two-dimensional horizontal plane. Simulations show the accuracy and feasibility of the proposed microphone array design in capturing a fully developed exterior soundfield.**

I. Introduction

Soundfield analysis based on spherical harmonic decomposition is widely utilised throughout audio acoustic applications of spatial soundfield recording [1], [2], [3], reproduction [4], [5], beamforming [6], [7] and source localization [8]. At the heart of these applications are the microphone and loudspeaker arrays used for three-dimensional (3D) spatial soundfield sampling and reconstruction. For 3D soundfield capture and reproduction, many types of array designs distributed on around a sphere have been proposed and implemented, such as designs of open [1], rigid [2], concentric [9], [10] and spherical shell [11] sensor arrays. Spherical arrays are ideal for 3D soundfield analysis as they are able to detect all spherical harmonic content of the soundfield which are an orthonormal set of spatial basis functions that can describe any function on the sphere. In practice, circular arrays are also common in cylindrical and planar geometric configurations as they offer greater feasibility over spherical arrays due to their flexible and scalable size. However planar arrays are traditionally unable to detect full 3D harmonic content from their measurements [12].

In [12], the authors used a planar array of pressure gradient microphones to capture interior 3D soundfields. A interior soundfield is a homogeneous soundfield observed over a spatial region which is caused by one or more sources located exterior to the region of interest. The underlying theory exploits the inherent properties of spherical harmonic functions and the omnidirectional pressure and pressure gradient measurements (pressure gradient with respect to the elevation angle) obtained by each array sampling position. This design manages to significantly reduce the minimum requirement of geometric sampling positions to capture a certain spatial soundfield while largely simplifying the array geometry.

In this paper, we propose a planar microphone array design and method for measuring a fully developed 3D exterior soundfield where an exterior soundfield is a homogeneous soundfield created by one or more sound sources located interior to the region of observation. The array consists of first-order (pressure gradient) microphones placed about concentric circles that lie purely in the soundfields horizontal plane. This allows for soundfield components which are normally undetectable by common planar omni-directional circular arrays to be captured in the horizontal plane through pressure gradient measurements. The proposed array is therefore able to achieve the planar geometric feasibility of circular arrays while maintaining the measurement capabilities of spherical microphone arrays.

The proposed method utilises three directions of pressure gradient measurement along with point pressure information to reduce the spatial sampling and hardware requirements of exterior soundfield capture. Algorithms to calculate the soundfield spherical harmonic coefficients are shown for arrays constructed of first-order microphones. Simulation and performance in capture and reconstruction of a hypothetical simple exterior soundfield is also presented.

II. Exterior Soundfield Measurements

A first order microphone provides four separate measurements, namely, pressure and pressure gradients along three orthogonal directions. In this section, we use spherical harmonics to expand these four components.

A. Harmonic Expansion of Exterior Soundfield

The spherical harmonic expansion of pressure for an exterior soundfield at a point (r, θ, ϕ) produced by a source at the origin O can be derived as [13]

$$S(r, \theta, \phi, k) = \sum_{n=0}^{N} \sum_{m=-n}^{n} \beta_{nm}(k) h_n(kr) Y_{nm}(\theta, \phi) \tag{1}$$

where r is the radial distance of the observation point for $r > r_s$, θ is the elevation angle for $0 \leq \theta \leq \pi$, ϕ is the azimuth angle for $0 \leq \phi \leq 2\pi$, $\beta_{nm}(k)$ are the modal (spherical harmonic) coefficients, $k = 2\pi f/c$ is the wave

ISBN 978-0-9928626-7-1

number, c is the speed of propagation, f is the frequency of the soundfield, N is the truncation order [14] of the exterior soundfield and is defined by $N = \lceil (ker_s/2) \rceil$ where r_s is the inner boundary of the exterior soundfield, $h_n(kr)$ is the spherical Hankel function of the first kind and $Y_{nm}(\theta, \phi)$ are the spherical harmonics, defined by [12]

$$Y_{nm}(\theta, \phi) = \mathbf{P}_{nm}(\cos\theta) e^{jm\phi} \tag{2}$$

where

$$\mathbf{P}_{nm}(\cos\theta) \equiv \sqrt{\frac{(2n+1)}{4\pi} \frac{(n-|m|)!}{(n+|m|)!}} p_{nm}(\cos\theta), \tag{3}$$

and $p_{nm}(\cdot)$ are the normalized associated Legendre functions and associated Legendre functions respectively. The set of orthogonal spherical harmonics are defined by the integers n for harmonic order and m for harmonic mode.

B. Omnidirectional Pressure Measurement

The omnidirectional pressure at a point within the horizontal plane $(r, \frac{\pi}{2}, \phi)$ of the exterior soundfield can be expressed using (1) as

$$S_{\text{omni}}\left(r, \frac{\pi}{2}, \phi, k\right) = \sum_{n=0}^{N} \sum_{m=-n}^{n} \beta_{nm}(k) h_n(kr) Y_{nm}\left(\frac{\pi}{2}, \phi\right) \tag{4}$$

C. Pressure Gradient Measurements

Soundfield pressure gradients with respect to the radial, azimuth and elevation directions at a point $(r, \frac{\pi}{2}, \phi)$ are defined by partial derivatives with respect to r, ϕ and θ:

$$S_{\text{diff}r}\left(r, \frac{\pi}{2}, \phi, k\right) = \sum_{n=0}^{N} \sum_{m=-n}^{n} \beta_{nm}(k) Y_{nm}\left(\frac{\pi}{2}, \phi\right) \times \left[\frac{1}{2}\left(h_{(n-1)}(kr) - \frac{h_n(kr) + (kr)h_{(n+1)}(kr)}{(kr)}\right) k\right] \tag{5}$$

$$S_{\text{diff}\phi}\left(r, \frac{\pi}{2}, \phi, k\right) = \sum_{n=0}^{N} \sum_{m=-n}^{n} \frac{jm}{r} \beta_{nm}(k) h_n(kr) Y_{nm}\left(\frac{\pi}{2}, \phi\right) \tag{6}$$

$$S_{\text{diff}\theta}\left(r, \frac{\pi}{2}, \phi, k\right) = \frac{-\sin\frac{\pi}{2}}{r} \sum_{n=0}^{N} \sum_{m=-n}^{n} \beta_{nm}(k) h_n(kr) \times \sqrt{\frac{(2n+1)(n^2-m^2)}{(2n-1)}} Y_{(n-1)m}\left(\frac{\pi}{2}, \phi\right). \tag{7}$$

D. Odd and Even Spherical Harmonic Components

Spherical harmonic coefficients can be separated into odd and even spherical harmonics when $(n + |m|)$ is either odd or even, respectively [15]. Measurements within the horizontal plane $(\theta = \pi/2)$ consists of either odd or even harmonics due to the properties of the normalised associate Legendre functions:

$$\mathbf{P}_{n|m|}\left(\cos\frac{\pi}{2}\right) = 0 \text{ for } (n + |m|) \text{ is odd} \tag{8}$$

$$\mathbf{P}_{(n-1)|m|}\left(\cos\frac{\pi}{2}\right) = 0 \text{ for } (n + |m|) \text{ is even.} \tag{9}$$

Using this property with the harmonic expansion of (4), (5) and (6), we observe that there are no odd harmonic components present within the pressure gradient measurements along radial (r) and azimuth (ϕ) directions. Whereas, from (7), we see that pressure gradient along the elevation direction contains only odd harmonic components. Thus, collectively using point pressure and 3 pressure gradients, we can measure quantities which contain full 3D soundfield information as the full set of spherical harmonic components can uniquely describe a 3D soundfield.

III. Estimation of Exterior Soundfield Coefficients

In this section, we show how to use first order microphones placed within a plane to approximate the exterior soundfield by way of estimating exterior soundfield coefficients $\beta_{nm}(k)$.

A. First Order Microphone Measurements

We express the first-order microphone measurements in terms of spherical harmonic coefficients with respect to the location of the microphone (i.e., local origin). Let $\alpha_{\nu\mu}^{(q)}(k)$, be the harmonic coefficients of the qth first order microphone within the measurement array with respect to its local origin and $(\nu, \mu) \in \{(0,0), (1,0), (1,-1), (1,1)\}$ represent the local harmonic order and mode. Thus, we have [16]

$$S_{\text{omni}}(r_q, \theta_q, \phi_q, k) = \alpha_{00}^{(q)}(k)\, j_0(0) Y_{00}(\theta, \phi) \tag{10}$$

$$S_{\text{diff}r}(r_q, \theta_q, \phi_q) = \left(\alpha_{1-1}^{(q)}(k) + \alpha_{1+1}^{(q)}\right) \left(\frac{k}{3}\right) Y_{1-1}\left(\frac{\pi}{2}, 0\right) \tag{11}$$

$$S_{\text{diff}\phi}(r_q, \theta_q, \phi_q) = \left(\alpha_{1-1}^{(q)}(k) - \alpha_{1+1}^{(q)}(k)\right) \left(\frac{k}{3}\right) Y_{1-1}\left(\frac{\pi}{2}, \frac{\pi}{2}\right) \tag{12}$$

$$S_{\text{diff}\theta}(r_q, \theta_q, \phi_q) = \left(\alpha_{10}^{(q)}(k)\right) \left(\frac{k}{3}\right) Y_{10}(\pi, \phi) \tag{13}$$

B. Exterior Soundfield Coefficients

Suppose Q first order microphones, each capable of measuring, pressure and three orthogonal pressure gradients, are located at positions $(r_q, \pi/2, \phi_q)$, $q = 1, \ldots, Q$ on a suitable plane which bisects the region that produces the exterior soundfield of interest. The co-ordinate system is chosen such that the plane is on the x-y plane. The output of each first order microphone is given by (4), (5), (6) and (7). By stacking the outputs of first order microphones, we obtain the following matrix equation:

$$\mathbf{S}(k) = \mathbf{X}(k)\mathbf{B}(k) \tag{14}$$

where

$$\mathbf{S}(k) = \begin{bmatrix} \mathbf{S}_{\text{omni}}(k) \\ \mathbf{S}_{\text{diff}r}(k) \\ \mathbf{S}_{\text{diff}\phi}(k) \\ \mathbf{S}_{\text{diff}\theta}(k) \end{bmatrix} \tag{15}$$

ISBN 978-0-9928626-7-1 © EURASIP 2017

are the set of point and gradient pressure measurements from the array with

$$\mathbf{S}_{\text{omni}}(k) = [S_{\text{omni}}(r_1, \pi/2, \phi_1, k), \cdots, S_{\text{omni}}(r_Q, \pi/2, \phi_Q, k)]^T$$
$$\mathbf{S}_{\text{diff}r}(k) = [S_{\text{diff}r}(r_1, \pi/2, \phi_1, k), \cdots, S_{\text{diff}r}(r_Q, \pi/2, \phi_Q, k)]^T$$
$$\mathbf{S}_{\text{diff}\phi}(k) = [S_{\text{diff}\phi}(r_1, \pi/2, \phi_1, k), \cdots, S_{\text{diff}\phi}(r_Q, \pi/2, \phi_Q, k)]^T$$
$$\mathbf{S}_{\text{diff}\theta}(k) = [S_{\text{diff}\theta}(r_1, \pi/2, \phi_1, k), \cdots, S_{\text{diff}\theta}(r_Q, \pi/2, \phi_Q, k)]^T,$$

$\mathbf{B}(k) = [\beta_{00}(k), \cdots, \beta_{NN}(k)]^T$ is the set of all exterior soundfield harmonic coefficients up to the system truncation order and

$$\mathbf{X}(k) = \begin{bmatrix} \mathbf{X}_{\text{omni}}(k) \\ \mathbf{X}_{\text{diff}r}(k) \\ \mathbf{X}_{\text{diff}\phi}(k) \\ \mathbf{X}_{\text{diff}\theta}(k) \end{bmatrix} \tag{16}$$

where each sub matrix is expressed in the form shown in (17) below. Each element of the solution matrix is related to each measurement type as expressed in (18), (19), (20) and (21).

$$\mathbf{X}_{\text{omni}}(k) = \begin{bmatrix} X_{00}^{\text{omni}}(1) & \dots & X_{nm}^{\text{omni}}(1) & \dots & X_{NN}^{\text{omni}}(1) \\ \vdots & \ddots & \vdots & \ddots & \vdots \\ X_{00}^{\text{omni}}(q) & \dots & X_{nm}^{\text{omni}}(q) & \dots & X_{NN}^{\text{omni}}(q) \\ \vdots & \ddots & \vdots & \ddots & \vdots \\ X_{00}^{\text{omni}}(Q) & \dots & X_{nm}^{\text{omni}}(Q) & \dots & X_{NN}^{\text{omni}}(Q) \end{bmatrix}, \tag{17}$$

$$X_{nm}^{\text{omni}}(q) = x_{nm}^{\text{omni}}\left(r_q, \frac{\pi}{2}, \phi_q, k\right) = h_n(kr_q) Y_{nm}\left(\frac{\pi}{2}, \phi_q\right) \tag{18}$$

$$X_{nm}^{\text{diff}r}(q) = x_{nm}^{\text{diff}r}\left(r_q, \frac{\pi}{2}, \phi_q, k\right) = Y_{nm}\left(\frac{\pi}{2}, \phi_q\right) \times \left[\frac{1}{2}\left(h_{(n-1)}(kr_q) - \frac{h_n(kr_q) + (kr_q)h_{(n+1)}(kr_q)}{(kr_q)}\right)k\right] \tag{19}$$

$$X_{nm}^{\text{diff}\phi}(q) = x_{nm}^{\text{diff}\phi}\left(r_q, \frac{\pi}{2}, \phi_q, k\right) = \frac{jm}{r_q} h_n(kr_q) Y_{nm}\left(\frac{\pi}{2}, \phi_q\right) \tag{20}$$

$$X_{nm}^{\text{diff}\theta}(q) = x_{nm}^{\text{diff}\theta}\left(r_q, \frac{\pi}{2}, \phi_q, k\right) = \frac{-\sin\frac{\pi}{2}}{r_q} h_n(kr_q) \times \sqrt{\frac{(2n+1)(n^2-m^2)}{(2n-1)}}\, Y_{(n-1)m}\left(\frac{\pi}{2}, \phi_q\right) \tag{21}$$

The exterior soundfield coefficients can then solved with a lest-squares solution and the pseudo inverse of $\mathbf{X}(k)$ [12], expressed as

$$\mathbf{B}(k) = \left(\mathbf{X}(k)^T \mathbf{X}(k)\right)^{-1} \mathbf{X}(k)^T \mathbf{S}(k). \tag{22}$$

IV. Array Configuration

This section describes restrictions that the proposed first-order microphone planar array must comply with to achieve complete three-dimensional exterior soundfield capture. The proposed measurement array consists of multiple concentric circles that are each comprised of evenly spaced first order microphones. The minimum number of first-order microphones within the array required for complete soundfield capture is defined as

$$Q \geq \frac{N(N+1)}{2} \tag{23}$$

where $N = \lceil ker_s/2 \rceil$ with r_s being the radius of a sphere encompassing all sources. This minimum number microphones is defined by the number of active odd harmonics within the soundfield. The minimum number of circles the measurement array must contain is defined by the number of zero mode odd harmonics within the soundfield. For complete soundfield capture the required minimum number of array circles is defined by C where

$$C \geq \left\lceil \frac{N}{2} \right\rceil \tag{24}$$

V. Simulations

In this section, we simulate the proposed two-dimensional horizontal array measurement method in application for capturing and reconstructing a full 3D exterior soundfield. The goal is to reconstruct the soundfield in a radial region of 0.5 to 2.5m for a frequency band of 200-8000 Hz. The soundfield is created with two point sources in positions $\left(0.1, \frac{\pi}{2}, 0\right)$ and $\left(0.1, \frac{\pi}{3}, 0\right)$ with respect to the global origin O. The frequency of the soundfield is simulated from 200 Hz to 10000 Hz.

A. Measurement Array

For a maximum target frequency of 8000 Hz and an inner soundfield boundary of 0.1 m, the system truncation order N is 20. Therefore, the measurement array must consist of at least 210 first order microphones spaced across 10 circles, determined from (23) and (24), respectively. The array configuration implemented for the simulation measurements uses these minimum requirements as shown in Fig.1.

B. Reconstructed Soundfield

The existing and reconstructed exterior soundfield are plotted in the radial range of 0.5 to 2.5 m for multiple conditions. The existing soundfield is simulated with the use of Green's equation and the two point source locations, expressed as

$$S(\bar{x}, k) = \frac{e^{ik||\bar{x}-\bar{x}_{s1}||}}{4\pi||\bar{x}-\bar{x}_{s1}||} + \frac{e^{ik||\bar{x}-\bar{x}_{s2}||}}{4\pi||\bar{x}-\bar{x}_{s2}||} \tag{25}$$

where $\bar{x}$ represents a location within the full 3D soundfield and $\bar{x}_s$ is the location of a omni-directional point source.

For the point source simulation operating at 800 Hz, Fig. 2 (a) and (b) show the existing and reconstructed soundfield at the $z = 0$ m plane and Fig. 2 (c) and (d) show the existing and reconstructed soundfield in the plane of $z = 1$ m. We observe that the existing and reconstructed soundfields

ISBN 978-0-9928626-7-1 © EURASIP 2017

are similar for operating frequencies below the measurement array's maximum frequency.

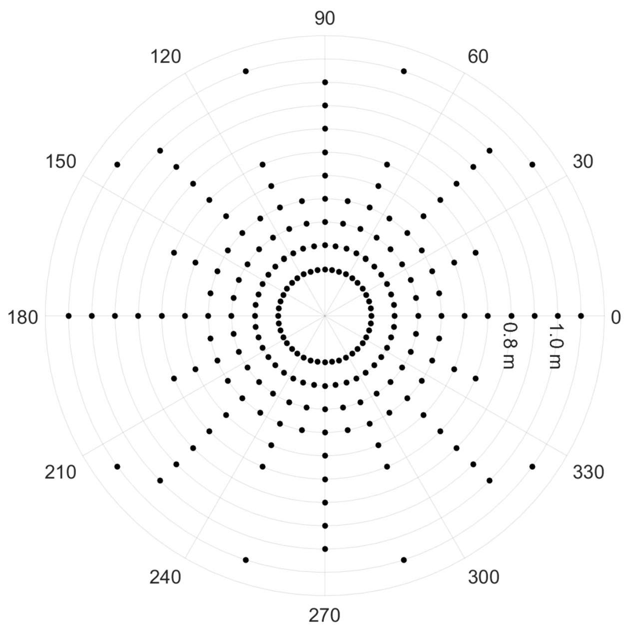

Fig. 1. Planar array configuration used for simulation example where the maximum frequency is 8000 Hz

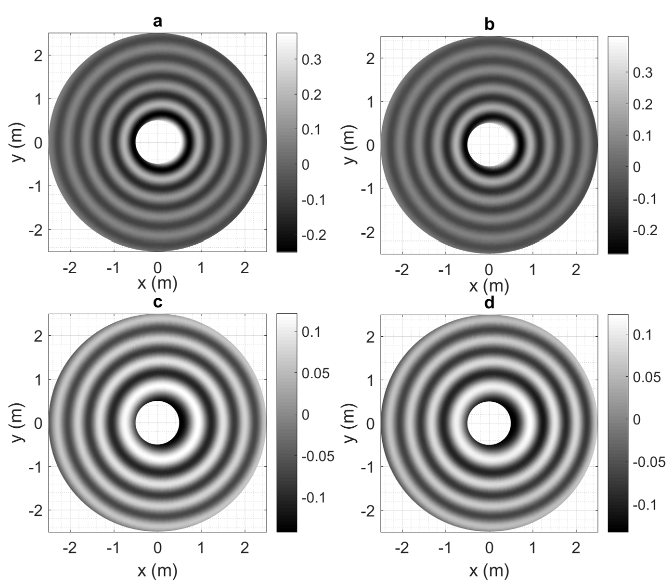

Fig. 2. Simulated soundfield at 800 Hz in (i) the $z = 0$m plane (a) existing and (b) reconstructed; (ii) the $z = 1$ m plane (c) existing and (d) reconstructed;

C. Exterior Soundfield Reconstruction Error

Fig.3 depicts the soundfield reconstruction error for a frequency range of $[200 : 10000]$ Hz and a radial range of 0.5 m to 2.5 m. Curves (a), (b) and (c) of Fig.3 are the average reconstruction error in the $z = 0$, $z = 0.3$ and $z = 1$ m planes, respectively. We observe that the horizontal plane error begins to increase significantly beyond a 8000 Hz, which is the desired maximum frequency of the measurement array. The $z = 1$ m plane however is observed to become erroneous well before the maximum design frequency at 2000 Hz. The $z = 0.3$ m plane is observed to have accuracy performance between these two other planes.

Curve (d) of Fig.3 shows the measurement performance of a equiangle spherical array with 256 sampling positions, designed for capture of a soundfield up to $N = 7$ and a frequency of 2800 Hz. In the plane of $z = 0.3$ m, it is observed that the planar and spherical array have similar performance for frequencies below 4000 Hz.

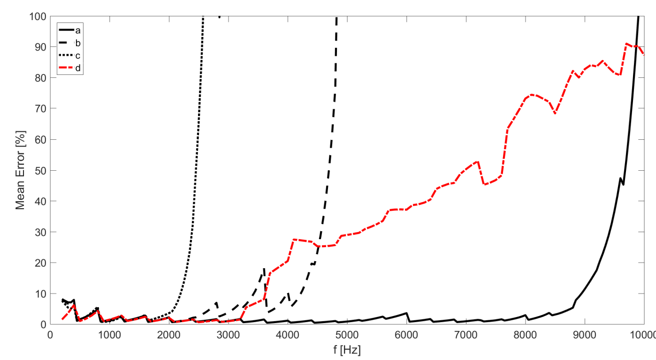

Fig. 3. Exterior soundfield reconstruction error in the (a) z = 0, (b) z = 0.3 m and (c) z = 1 m planes for a planar array; (d) z = 0.3 m plane for a spherical array

Fig.4 depicts locations of high soundfield reproduction error for capture performed by the proposed planar array in (a) and a similarly sized spherical array with 256 sampling positions in (b). Reproduction in the $z = 0.3$ m plane with the planar array is observed to have erroneous regions concentrated near the system z-axis. These results suggest that captured error in the planar measurement method is introduced through poor estimation of zero mode harmonic coefficients, as they are present in the z-axis. Results from Fig.3 however, suggest that even harmonic coefficients (including those of zero mode) are accurately estimated by the planar array as the purely even soundfield in the $z = 0$ m plane is successfully reproduced.

VI. Error and Accuracy Analysis

Addressed here are sources of error in the proposed exterior soundfield measurement method and their influences on harmonic coefficient estimation accuracy.

A. Improved Odd Soundfield Spatial Sampling

The previous simulation shows a measurement array designed with the minimum number of high-order microphones required to completely capture the existing exterior soundfield. This minimum number is used to achieve a solution matrix $\mathbf{X}(k)$ with a full rank, such that $\mathbf{X}_{\text{diff}\theta}(k)$ is square.

Utilizing a minimum number of sensors like this is not common in applications of 3D spherical measurement arrays. Spatial sampling techniques such as equiangle and Gaussian

ISBN 978-0-9928626-7-1

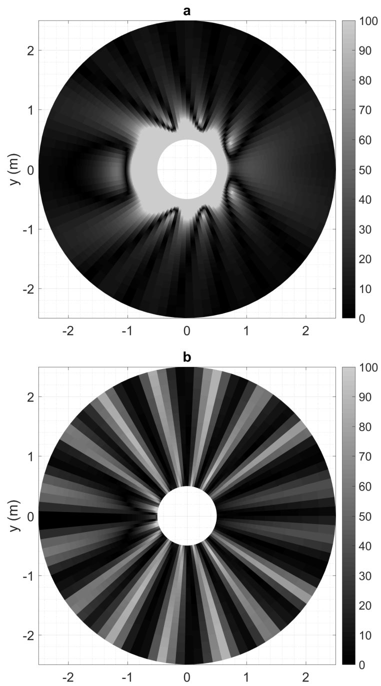

Fig. 4. Soundfield reproduction error at 5000 Hz in the z = 0.3 m plane, truncated to 100% from measurements of (a) first order planar array and (b) spherical array

[17] use a number of microphones greater than the number of active soundfield harmonics. Therefore utilising a greater number of microphones than expressed by (23) within the proposed array will increase the accuracy of soundfield capture. In a similar vein, increasing the number of concentric circles within the array would be expected to improve zero mode coefficient estimation.

The improvements gained from increasing planar array size can be observed within Fig.3, where the proposed array of 210 sensors can be considered as an array with a sensor count chosen from $Q \geq 4\left(\frac{N(N+1)}{2}\right)$ for a target order of $N = 9$. For the simulation, this measurement target corresponds to a maximum capture frequency of roughly 3600 Hz.

B. Truncation Error

Spherical harmonic aliasing will occur for soundfields operating at frequencies above a microphone array's designed maximum. This is due to the soundfield content of orders $n \leq N$ being aliased by higher-orders.

For soundfields operating at frequencies below the microphones design maximum, it is observed that the reproduction error fluctuates between 1-5%. This result agrees with the expected error of 4% [4] for reproducing soundfields from a set of truncated spherical harmonic coefficients.

VII. Conclusion

This paper proposes a novel method to capturing 3D exterior soundfields using an array of first order microphones located on a plane. Such an array provides many practical applications and would be preferred over using a large spherical array that has to encompass all sources. First order microphones are placed within a concentric circular two-dimensional planar array, allowing the proposed design to measure soundfield components in the horizontal plane that are undetectable to omni-directional microphones.

Acknowledgment

This work is supported by Australian Research Council (ARC) Discovery Project DP140103412.

References

[1] T. D. Abhayapala and D. B. Ward, "Theory and design of high order sound field microphones using spherical microphone array," in *IEEE International Conference on Acoustics, Speech and Signal Processing (ICASSP)*, May 2002.

[2] J. Meyer and G. Elko, "A highly scalable spherical microphone array based on an orthonormal decomposition of the soundfield," in *IEEE International Conference on Acoustics, Speech and Signal Processing (ICASSP)*, May 2002.

[3] Y. Peled and B. Rafaely, "Method for dereverberation and noise reduction using spherical microphone arrays," in *IEEE International Conference on Acoustics, Speech and Signal Processing (ICASSP)*, March 2010.

[4] D.B. Ward and T.D. Abhayapala. "Reproduction of a plane-wave sound field using an array of loudspeakers." *IEEE Transactions on speech and audio processing*, 9.6 (2001): 697-707.

[5] A. Gupta and T. D. Abhayapala, "Three-dimensional sound field reproduction using multiple circular loudspeaker arrays," *IEEE Transactions on Audio, Speech, and Language Processing*, vol. 19, pp. 1149-1159, Oct. 2010.

[6] E. Tiana-Roig, F. Jacobsen and E. Fernandez-Grande, "Beamforming with a circular array of microphones mounted on a rigid sphere (L)," The Journal of the Acoustical Society of America, vol. 130, pp. 1095-198, Jul. 2011.

[7] S. Yan, H. Sun, U. Svensson, X. Ma and J. Hovem, "Optimal modal beamforming for spherical microphone arrays," IEEE Transactions on Audio, Speech, and Language Processing, vol. 19, pp. 361-371, Apr. 2010.

[8] S. Argentieri, P. Danes and P. Soueres, "Modal analysis beamforming for nearfield or farfield speaker localization in robotics," in International Conference on Intelligent Robots and Systems, October 2006.

[9] A. Parthy, C. Jin, and A. Schaik. "Acoustic holography with a concentric rigid and open spherical microphone array", *IEEE International Conference on Acoustics, Speech and Signal Processing (ICASSP)*, 2009.

[10] T. D. Abhayapala and M. C. T. Chan, "Limitation and errior analysis of spherical microphone arrays" *14th International Congress on Sound and Vibration (ICSV14)*, 2007.

[11] I. Balmages and B. Rafaely, "Open-sphere designs for spherical microphone arrays," IEEE Transactions on Audio, Speech, and Language Processing, vol. 15, pp. 727-732, Jan. 2007.

[12] H. Chen, T. D. Abhayapala and W. Zhang, "Theory and design of compact hybrid microphone arrays on two-dimensional planes for three-dimensional soundfield analysis," The Journal of the Acoustical Society of America, vol. 138, pp. 3081-3092, Nov. 2015.

[13] P. N. Samarasinghe and T. D. Abhayapala, "Room transfer function measurement from a directional loudspeaker," in International Workshop on Acoustic Signal Enhancement (IWAENC), September 2016.

[14] R. A. Kennedy, P. Sadeghi, T. D. Abhayapala and H. M. Jones, "Intrinsic limits of dimensionality and richness in random multipath fields," IEEE Transactions on Signal Processing, vol. 55, pp. 2542-2556, May. 2007.

[15] T. D. Abhayapala, A. Gupta, "Spherical harmonic analysis of wavefields using multiple circular arrays," IEEE Transactions on Audio, Speech, and Language Processing, vol. 18, pp. 1655-1666, Aug. 2010.

[16] H. Chen, T. D. Abhayapala, P. N. Samarasinghe and W. Zhang, "Direct-to-reverberant energy ratio estimation using a first order microphone," IEEE/ACM Transactions on Audio, Speech, and Language Processing, vol. 25, pp. 226-237, Feb. 2017.

[17] B. Rafaely, "Analysis and design of spherical microphone arrays," IEEE Transactions on Speech and Audio Processing, vol. 13, pp. 1063-6673, Jan. 2005.